# Geometrical Similarities of the Orlov and Tuy Sampling Criteria and a Numerical Algorithm for Assessing Sampling Completeness

S.D. Metzler, *Member, IEEE,* J.E. Bowsher, *Member, IEEE,* and R.J. Jaszczak, *Fellow, IEEE*

***Abstract*— Tuy and others have derived a sufficiency condition for complete sampling using a cone-beam geometry. Herein, we express Tuy's cone-beam condition in the language and geometry of Orlov's condition for parallel-beam collimation. One may determine from this condition what volume is completely sampled. This inversion has been implemented in software. The software determines a lower bound on the completely sampled volume for arbitrary orbits.**

***Index Terms*— Orlov, Tuy, Data Sufficiency, Conebeam, Pinhole, Parallel-beam**

## I. Introduction

ORLOV'S condition is based on the set of vantage angles observed by parallel-beam collimation [1]. Tuy's condition is a condition on the relationship of points to the curve of the cone-beam's focal (source) point [2]. Tuy's condition is equivalent to Orlov's condition in the limit of in nite focal length [3]. We develop this relationship further by highlighting a geometrical similarity between Tuy's condition and Orlov's.

## II. Sampling Criteria

### A. Sampling Criteria for Parallel-Beam Collimation

Orlov derived in the context of electron microscopy the complete-sampling condition for three-dimensional reconstruction from parallel projection data [1]. He stated his condition geometrically: the curve of vantage angles on a unit sphere of directions must "have points in common with any arc of a great circle [1]." Orlov's condition was derived based on the assumption that the entire density function $f(x)$ is observed from the same set of vantage angles (i.e., untruncated parallel-beam collimation). Hence, one can use Orlov's condition to determine the completely sampled volume for a given parallel-beam orbit as follows: Determine the set of points that are untruncated throughout the orbit and then apply Orlov's criterion to the set of view angles for any point within that volume. Since parallel-beam collimators have translational symmetry (i.e., shift invariance), all points in the untruncated volume are seen by the same set of vantage angles. Orlov's criteria is a condition on the set of vantage angles seen by all points.

S. D. Metzler and J.E. Bowsher are with the Department of Radiology at Duke University Medical Center, Durham, NC. R. J. Jaszczak is with the Department of Radiology at Duke University Medical Center, Durham, NC, and with the Department of Biomedical Engineering at Duke University, Durham, NC.

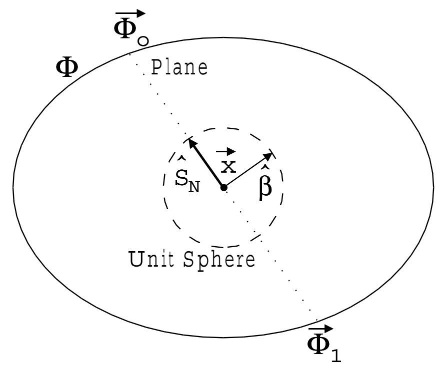


Fig. 1. A plane (dotted line) with normal $\hat{\beta}$ intersects the object at $\vec{x}$. The plane also intersects the path $\Phi$ of the focal-point curve (solid ellipse) at $\vec{\Phi}_0$ and $\vec{\Phi}_1$. The unit vector of the vantage angle is $\hat{S_N}$. The unit sphere of directions (indicated by the dashed circle) is centered at $\vec{x}$. The unit direction vectors $\hat{\beta}$ and $\hat{S_N}$ have their origin at $\vec{x}$.

### B. Sampling Criteria for Cone-beam Collimation

Tuy and others have derived a completeness condition for cone-beam acquisitions [2], [4], [5]. The Tuy condition is also stated geometrically: "if on every plane that intersects the object there exists at least one cone-beam source (focal) point, then one can reconstruct the object [2], [5]."

Cone-beam collimation approaches the translational invariance of parallel-beam collimation in the limit of in nite focal length. However, when the focal length is nite, the translational symmetry of the cone-beam collimator is broken. Consequently, the set of vantage angles provided by a given orbit varies from one point to another.

### C. Generalization of Orlov's Sampling Criterion

We now attempt to geometrically connect Orlov's condition to the Tuy condition. Fig. 1 depicts the Tuy condition at point $\vec{x}$ in the completely sampled volume. One plane through the point is indicated by the dotted line; its normal is unit vector $\hat{\beta}$. The curve of focal points $\Phi$ is represented as a solid ellipse. The curve intersects the plane at $\vec{\Phi}_0$ and $\vec{\Phi}_1$. The Tuy condition requires the curve to intersect the plane through $\vec{x}$ corresponding to each possible value (direction) of unit vector $\hat{\beta}$. Although there may be multiple intersections, only one is needed: $\vec{\Phi}_0$.

0-7803-7636-6/03/$17.00 ©2003 IEEE.

Orlov's condition is based on the set of angles from which $f(x)$ is viewed. The vantage angle $\vec{S}$ is the vector from $\vec{x}$ to $\vec{\Phi_0}$. $\hat{S_N}$ is the normalized (unit) vantage angle.

To establish the connection between Orlov's condition and Tuy's condition, we introduce two orthonormal basis vectors $\hat{b_1}$ and $\hat{b_2}$ such that

$$\hat{\beta} \cdot \hat{b_1} = 0, \hat{\beta} \cdot \hat{b_2} = 0, \hat{b_1} \cdot \hat{b_2} = 0, \text{ and } |\hat{b_1}| = |\hat{b_2}| = 1. \quad (1)$$

The vector $\vec{x}$ may be parameterized as

$$\vec{x} = (\vec{x} \cdot \hat{\beta})\hat{\beta} + (\vec{x} \cdot \hat{b_1})\hat{b_1} + (\vec{x} \cdot \hat{b_2})\hat{b_2}, \quad (2)$$

and the points on the plane through $\vec{x}$ whose normal is $\hat{\beta}$ may then be parameterized as

$$\vec{P} = (\vec{x} \cdot \hat{\beta})\hat{\beta} + k_1\hat{b_1} + k_2\hat{b_2}, \quad (3)$$

where $k_1$ and $k_2$ range over all real numbers.

The intersection of the plane $\vec{P}$ with the curve $\Phi(\lambda)$ occurs at $\vec{\Phi}_0$.

$$\vec{\Phi_0} = (\vec{x} \cdot \hat{\beta})\hat{\beta} + (\vec{\Phi}_0 \cdot \hat{b_1})\hat{b_1} + (\vec{\Phi}_0 \cdot \hat{b_2})\hat{b_2} \quad (4)$$

The vantage angle, $\vec{S}$, is the vector from $\vec{x}$ to $\vec{\Phi}_0$.

$$\vec{S} = \vec{\Phi}_0 - \vec{x} = \left[\vec{\Phi}_0 \cdot \hat{b_1} - \vec{x} \cdot \hat{b_1}\right] \hat{b_1} + \left[\vec{\Phi}_0 \cdot \hat{b_2} - \vec{x} \cdot \hat{b_2}\right] \hat{b_2}. \quad (5)$$

The normalized vantage angle is

$$\hat{S_N} = \frac{\vec{S}}{|\vec{S}|}. \quad (6)$$

The vantage angle is perpendicular to $\hat{\beta}$ because $\hat{b_1}$ and $\hat{b_2}$ are perpendicular to $\hat{\beta}$ (eq. 1); the $\hat{\beta}$ component of $\hat{S_N}$ is zero. Since $\hat{S_N}$ is perpendicular to $\hat{\beta}$ and its origin is $\vec{x}$, it is contained in the plane $\vec{P}$.

Each great circle is the intersection of a sphere with a plane that contains the center of the sphere. There is a one-to-one mapping between unit great circles centered at $\vec{x}$ and planes $(\vec{x} \cdot \hat{\beta}, \hat{\beta})$ where the ordered pair $(\vec{x} \cdot \hat{\beta}, \hat{\beta})$ uniquely speci es a plane by its normal $\hat{\beta}$ and its displacement from the origin $\vec{x} \cdot \hat{\beta}$ along the direction $\hat{\beta}$. If the curve of focal points has multiple intersections, all intersections correspond degenerately to the same plane and great circle.

If a plane de ned by $\hat{\beta}$ and $\vec{x} \cdot \hat{\beta}$ intersects the curve of the focal point $\vec{\Phi}$, then the corresponding great circle is intersected by the direction vector $\hat{S_N}$ specifying the view angle. The great circle is in the plane $\vec{P}$ and its center is $\vec{x}$. The vector $\hat{S_N}$ is a vector in the plane $\vec{P}$ with origin $\vec{x}$. Since the great circle and $\hat{S_N}$ are in the same plane, they both share the same origin, and the magnitude of $\hat{S_N}$ equals the circle's radius, $\hat{S_N}$ is the displacement vector from $\vec{x}$ to a point on the great circle de ned by $\hat{\beta}$. Consequently, if a plane through $\vec{x}$ intersects the curve of focal points, the corresponding great circle is also intersected. Therefore, for all planes to intersect the focal curve, all great circles must be intersected and for all great circles to be intersected, all planes through $\vec{x}$ must intersect the focal curve.

Tuy's condition [2] may be stated as follows, using the geometrical language of Orlov: The set of vantage angles on a unit sphere of directions, from each voxel to each point on the curve of focal points, must "have points in common with any arc of a great circle [1]" surrounding that voxel. Based on this restatement of Tuy's condition, we introduce a numerical algorithm for determining the largest completely sampled region (LCSR) corresponding to a given cone-beam or parallel-beam orbit. Let the support be the set of voxels over which the imaged object $f(x)$ may be non-zero (i.e., $f(x)$ is known to be zero outside the support.) In analogy to the *universal aperture* concept for parallel-beam collimation [3], we de ne the *universal aperture* for cone-beam collimation for a region of space $B$ to be the set of focal points for which $B$ is not truncated. In the limit of in nite focal length (parallel-beam collimation), this is equivalent to the set of projection directions for which $B$ is not truncated since all voxels within the support experience the same view angle. We consider only projection views that are in the *universal aperture* of the support; $B$ corresponds to the support. This assures that the object is untruncated (since the object is zero outside the support) for all views that are considered (all views in the universal aperture). Both the Tuy and Orlov conditions require that there be no truncation. We de ne the LCSR to be the largest subset of the support that is completely sampled by the universal aperture. The LCSR is the subset of points that meet Tuy's condition. Since the non-zero voxels are contained within the support, the density function can be reconstructed within the LCSR [2].

## III. Algorithm for Calculating Completely Sampled Volumes

An algorithm has been developed to determine the LCSR. A voxelized representation of the volume to evaluate is created. Then a set of collimator models is constructed to simulate the positions, orientations and spatial extents of the collimators. For example, a single parallel-beam collimator following an orbit that includes $m$ projection views would be represented by $m$ collimator models. Two collimators with $m$ and $n$ projection views, respectively, would be represented by $m + n$ collimator models. For each voxel, a digitized version of the vantage points of the voxel are determined from the set of collimator models. The digitized vantage curve (DVC) is then evaluated to determine if any great circles can exist on the Orlov sphere without intersecting the vantage curve.

This algorithm has been implemented in C++ using Object-Oriented programming techniques [6]. When started, the program allocates and initializes a boolean matrix representing the voxelized volume to consider. It then reads one or several orbit les and constructs a set of collimator representations. All detector representations obey an *abstract interface* that determines if a given voxel is within the eld-of-vie w of the collimator and the vantage angles for that voxel [6].

The use of an abstract interface makes it possible to model multiple collimator types simultaneously and extend the program to consider new collimator types without any change to the algorithm. The new collimator simply needs to implement this interface.

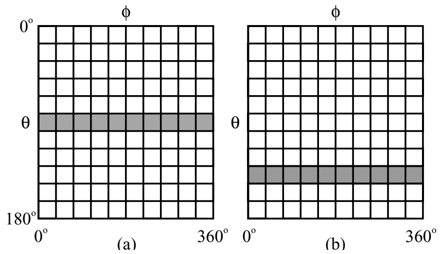


Fig. 2. Digital representation of vantage curves. The digital representations of the vantage curves for a 360° orbit of a parallel-beam collimator and a slant-hole collimator are shown schematically as matrices in (a) and (b), respectively. Observed vantage points (OVP) are shaded. Unobserved vantage points (UVP) are unshaded. The equator in (a) is shaded, but completely unshaded in (b).

### A. Vantage Curve Digitization

The DVC for each voxel is fully determined and evaluated before the next voxel is considered in order to reduce the required memory. The vantage curve is stored in digital form by using a two-dimensional grid to represent the polar angle, $\theta$, and the azimuthal angle, $\phi$, of each vantage point. The grid is boolean so that *true* represents a coordinate pair for an observed vantage point (OVP) and *false* represents an unobserved vantage point (UVP). An odd, but variable, number of rows ($N_{\mathrm{rows}}$) were used to represent $\theta$ so that the central row corresponded to the equator. An even number of columns ($N_{\mathrm{cols}}$) represented $\phi$ for the matrix so that each column has a well-de ned complementary column (CC), which represents the azimuthal values on the opposite side of the sphere. The CC is 180° and $N_{\mathrm{cols}}/2$ bins away from its pair. A schematic representation of a DVC is shown in Fig. 2.

### B. Vantage Curve Evaluation

After all the projection views have been considered for a voxel, the vantage curve is complete and is evaluated to determine if any great circles can exist on the sphere without intersecting the vantage curve. The parameterization of a generic great circle (Fig. 3) can be found by considering that the points with the minimum and maximum $z$ values are

$$\hat{r}_{\max} = (\sin\theta_{\mathrm{m}}\cos\phi_{\mathrm{m}}, \sin\theta_{\mathrm{m}}\sin\phi_{\mathrm{m}}, \cos\theta_{\mathrm{m}})$$
$$\hat{r}_{\min} = (-\sin\theta_{\mathrm{m}}\cos\phi_{\mathrm{m}}, -\sin\theta_{\mathrm{m}}\sin\phi_{\mathrm{m}}, -\cos\theta_{\mathrm{m}}), \qquad (7)$$

where $\theta_{\mathrm{m}}$ is the value of $\theta$ for the circle's maximum $z$ point.

A normal to the circle can be parameterized as

$$\hat{N} = (\cos\theta_{\mathrm{m}}\cos\phi_{\mathrm{m}}, \cos\theta_{\mathrm{m}}\sin\phi_{\mathrm{m}}, -\sin\theta_{\mathrm{m}}). \qquad (8)$$

The normal can be used to determine the basis vector orthogonal to $\hat{r}_{\max}$, $\hat{r}_{\min}$, and $\hat{N}$.

$$\hat{b} = \hat{r}_{\max} \times \hat{N} = -\hat{x}\sin\phi_{\mathrm{m}} + \hat{y}\cos\phi_{\mathrm{m}} \qquad (9)$$

Any point on the great circle can be parameterized as

$$\hat{r} = \alpha\hat{r}_{\max} + \beta\hat{b}. \qquad (10)$$

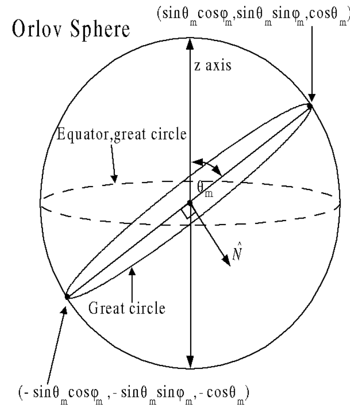


Fig. 3. Generic great circle on an Orlov sphere. The point $(\sin\theta_{\mathrm{m}}\cos\phi_{\mathrm{m}}, \sin\theta_{\mathrm{m}}\sin\phi_{\mathrm{m}}, \cos\theta_{\mathrm{m}})$ has the maximum value of $z$ on this curve. The point $(-\sin\theta_{\mathrm{m}}\cos\phi_{\mathrm{m}}, -\sin\theta_{\mathrm{m}}\sin\phi_{\mathrm{m}}, -\cos\theta_{\mathrm{m}})$ has the minimal value of $z$ on this curve. The normal to the plane of this great circle is $\hat{N}$.

Since $|\hat{r}| = |\hat{r}_{\max}| = |\hat{b}| = 1$, and $\hat{r}_{\max}$ and $\hat{b}$ are orthogonal,

$$\alpha^2 + \beta^2 = 1. \qquad (11)$$

Letting $\alpha = \cos\gamma$ and $\beta = \sin\gamma$,

$$\hat{r} = (\cos\gamma\sin\theta_{\mathrm{m}}\cos\phi_{\mathrm{m}} - \sin\gamma\sin\phi_{\mathrm{m}},$$
$$\cos\gamma\sin\theta_{\mathrm{m}}\sin\phi_{\mathrm{m}} + \sin\gamma\cos\phi_{\mathrm{m}}, \cos\gamma\cos\theta_{\mathrm{m}}), \qquad (12)$$

where $\theta_{\mathrm{m}}$ and $\phi_{\mathrm{m}}$ are the coordinates of the point of maximum $z$ on the curve and $\gamma$ parameterizes the curve.

Equation 12 is used to evaluate if any great circles can exist on the sphere without intersecting the vantage curve. The matrix representing the DVC is evaluated by using each element in the top half of the matrix ($\theta < 90°$) as $\hat{r}_{\max}$ for a particular trial great circle. Equation 12 is then used to determine all the other element locations that are on the same trial great circle by varying $\gamma$. The element locations are compared with the OVPs to determine if there are intersections. If an intersection is found, the trial great circle is not allowed and the next trial great circle is checked by choosing the next $\hat{r}_{\max}$.

Although equation 12 gives the form of the generic great circle, it can be computationally intensive to apply to all points on the digitized curve using the method described above. Several simpli ed cases are checked before the generic method is used. First, the number of OVPs found must be greater than the smaller of $N_{\mathrm{rows}}$ and $N_{\mathrm{cols}}/2$. Otherwise a great circle can be drawn. Second, the equator is checked to verify that a great circle cannot be drawn through the equator. This check is satis ed if a single observed point is found (Fig. 2b fails this check.). Third, the azimuthal columns are checked to verify that a great circle cannot be drawn longitudinally. This check is satis ed if a single observed point is found in a column or its CC. Fourth, the central row (equator) is checked to see if enough of it is lled in to exclude all great circles. This last case would require that a contiguous section of the equator at least as large as half of the circumference be marked as observed (Fig. 2a passes this check.).

0-7803-7636-6/03/$17.00 ©2003 IEEE.

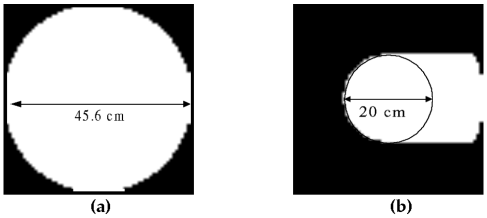


Fig. 4. Transaxial slice of the LCSR for parallel-beam collimator with a circular orbit. The volume is cylindrical with a diameter of 45.6 cm.

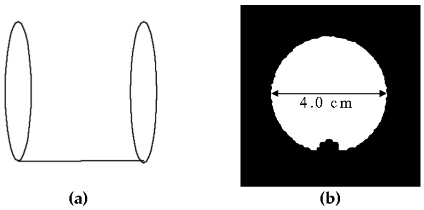


Fig. 5. Orbit ((a); left) of the focal point of a cone-beam/pinhole collimator and transaxial slice ((b); right) of the LCSR for that orbit.

### C. Examples

The program has been tested using parallel-beam collimators, slant-hole collimators, and cone-beam/pinhole collimators. Example volumes are described below.

*1) Parallel-Beam Collimators with Circular Orbits:* Parallel-beam collimators with untilted circular 360° orbits have been evaluated on a $64^3$ grid of 0.712-cm-wide voxels and give cylindrical LCSRs, as expected. A transaxial slice of an LCSR is shown in Fig. 4(a). For this LCSR, the gamma camera dimensions were 45.6 cm transaxially and 22.8 cm axially. The radius of rotation was 30.0 cm.

The LCSR of a parallel-beam collimator following a circular orbit depends only on the detector dimensions and not the orbit dimensions. That volume is cylindrical with magnitude $\pi w^2 d/4$, where $w$ is the transaxial width of the detector and $d$ is the axial depth of the detector. The volume predicted by the formula is 37,157 cm$^3$. The volume determined by the program was 38,670 cm$^3$, which is larger than expected by 4%, presumably because of binning effects.

Fig. 4(b) shows the LCSR for a semicircular (180°) orbit of a parallel-beam collimator. It is asymmetric. Halfway through the 180° orbit, the camera has a view to the right. The ROR was 10.0 cm. The calculated volume was 14,761 cm$^3$. The expected volume was

$$\frac{w^2}{4}\sin^{-1}\frac{20}{w}+\frac{20}{4}\sqrt{w^2-20^2}+\frac{20^2}{8}\pi=13,634\ \mathrm{cm}^3. \quad (13)$$

*2) Cone-beam/Pinhole Collimators:* A cone-beam/pinhole collimator model has been implemented for the algorithm. A collimator with an opening angle of 180° has been tested with a pair of 128-view circular orbits (ROR=2.0 cm), separated axially by 4.0 cm. The pair is connected by the 4.0 cm linear translation of the focal point. The orbit (left) and the volume are shown in Fig. 5. It is the closest to the focal point during the axial translation. The calculated volume is 48.5 cm$^3$, compared

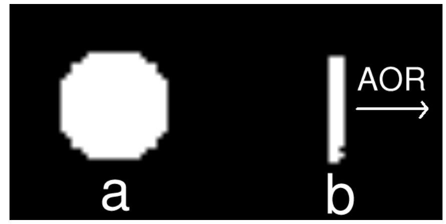


Fig. 6. LCSR for spiral pinhole-collimator orbit. Transaxial (a) and sagittal (b) slices through the LCSR are shown. The volume is nearly cylindrical, except for defects at the ends (b, bottom), where the valid volume depends on the initial angle of acquisition, and except for binning effects. The axial translation of the orbit is 1.28 cm, which corresponds to two bins. The volume is three bins wide axially due to edge effects and centering.

with the 50.3 cm$^3$ volume of the cylinder outlined by the orbit. Much of the difference is due to the defect at the bottom of the LCSR, nearest the axial translation of the focal point. This defect is due to the nite steps of the orbit and binning effects. The pinhole-collimator has also been tested with a 192-view spiral orbit and gives a nearly cylindrical volume using a $64^3$ grid of 0.712 cm-wide voxels (Fig. 6). The orbit included a 128-view spiral orbit with a 10 cm ROR traversing 1.28 cm along the axis of rotation followed by a 64-view half-circular orbit at the far end of the spiral. The defects in the cylinder are at the ends, as expected because of the strong dependence on the initial orientation of the camera. The total volume determined by the program was 368 cm$^3$.

## IV. Discussion

The completeness condition for ideal parallel-beam collimators may be evaluated at a single point because of the symmetry of the collimator. For parallel-beam collimators, the set of vantage angles is the same for all points in the untruncated volume; there is translational invariance in parallel-beam collimation. Cone-beam collimation breaks the symmetry of the parallel-beam collimator resulting in a point-wise completeness condition. Tuy's condition at a point has been shown to be geometrically equivalent to the following condition: the curve of vantage angles on a unit sphere of directions centered on that point must "have points in common with any arc of a great circle [1]." Tuy's condition is equivalent to the point-wise application of Orlov's condition. The geometrical language of Orlov is employed here as the basis for a numerical algorithm that assesses the volume over which Tuy's condition is met.

The LCSR is the region that is completely sampled by a set of projections. Since all non-zero activity is within the support and only untruncated views are used, the activity distribution within the LCSR may be reconstructed from the projections. The algorithm presented in this paper determines the volume of completely sampled points. An alternative to this algorithm would be to consider the common volume (i.e., the volume that is not truncated by any projection views) and then determine the LCSR as a subset of the common volume. In this formulation, all non-zero activity would need to be contained within the common volume so that the LCSR can be reconstructed [2]. A disadvantage of this alternative algorithm is that the common volume may be severely limited by a small number of projection views.

The current algorithm has successfully determined the LCSR in cases that are easily veri ed intuitively. It has been used to study the more complex scenarios of pinhole collimators following a helical orbit. This technique may be useful for studying complete orbits and understanding sampling artifacts for complex projection acquisitions.

Algorithm optimization has been an important issue for timely completion of the volume calculation. For the $64^3$ voxel representation used herein, the approximate computation time on an AMD 1.0 GHz processor is 5 minutes, but is sensitive to the complexity of the orbit. This time is typically dominated by evaluations that require the full use of equation 12 instead of one of the simpler evaluations that were mentioned in the same section. One optimization would be to apply the test to parallel-beam data at just one point in the untruncated volume. However, this would break the abstraction model of the program for only a factor of 2 gain in performace. It may then be dif cult to evaluate complete sampling for mixed collimation. Further optimizations would involve improving the implementation of the check using equation 12. One way this could be done would be to pre-compute the great circles for each row of the matrix. Since the columns represent equally spaced azimuthal regions, the curve can then be translated quickly on the y . It is also possible that other simplifying cases can be added to more quickly evaluate for great circles. These additional optimizations are not currently a signi cant issue because of the fast computation time that has already been achieved.

Orlov's condition assumes continuous angular sampling and in nitesimal sampling bins. Both of these conditions are invalid in realistic acquisitions. By Nyquist's theorem, there are limitations in reconstruction resolution due to discrete sampling. The algorithm described herein uses a discrete matrix to determine the DVC and hence the LCSR. The size of the grid needs to match the angular sampling of the orbit. If the matrix is too small, the algorithm determines the LCSR for too small of a Nyquist frequency. If it is too large, there would be UVPs, allowing great circles to be drawn where they should not be.

A more sophisticated solution is to use a large matrix in the DVC and to connect points that are within a certain distance on the unit sphere calculated from a user-speci ed sampling frequency or the Nyquist frequency. This technique would require signi cantly longer computation times using the current evaluation algorithm. However, additional optimizations could be made to the algorithm to improve performance. Moreover, this technique would allow the LCSR to be determined as a function of sampling frequency, showing which regions of the volume would have better sampling than others.

By using the point-wise Orlov condition, it may be possible to determine if the composite sampling from different collimator types is complete even if the individual sampling from each collimator is not complete. Since parallel-beam collimators are cone-beam collimators with in nite focal length (Cone-beam collimators are not parallel-beam collimators.), it seems reasonable, although unproven as far as we know, that combined orbits of parallel-beam and cone-beam collimation can be evaluated by the generalized (point-wise) Orlov condition. However, since parallel-beam collimation measures plane integrals, all of which must be measured to invert the Radon transform [8], and cone-beam collimation measures the derivative of the transform [9], there is also reason to believe that this method may not be correct for mixed collimation.

This technique for computing the LCSR for SPECT acquisitions may be applied to CT acquisitions without modi cation to the algorithm. For CT, the line integral of attenuation is sampled at a set of positions. By adding a new collimator type to the program, the voxels seen during a particular view may be determined. For each sampled voxel, the direction of the photon beam that samples it would be recorded as the vantage direction. The rest of the program would work without change.

## V. Conclusion

Tuy's condition is geometrically equivalent to the following condition: The set of vantage angles on a unit sphere of directions, from each voxel to each point on the curve of focal points, must "have points in common with any arc of a great circle [1]" surrounding that voxel. This is equivalent to requiring every point in the support to meet the geometrical condition stated by Orlov for the case of parallel-beam collimation. Orlov's condition, as derived and written, cannot be applied to cone-beam collimation because it assumes that every point sees the same set of view angles; in cone-beam collimation every point sees a different set of view angles.

An algorithm based on this point-wise Orlov condition has been described. The algorithm determines the completely sampled volume. Examples of its application have been shown. The examples agree with expectation in all cases that can be easily determined analytically.

## References


[1] S.S. Orlov, "Theory of three dimensional reconstruction. I. Conditions for a complete set of projections," *Sov. Phys. Crystallogr.*, vol. 20, no. 3., pp. 312–314, 1975.

[2] H.K. Tuy, "An Inversion Formula for Cone-Beam Reconstruction," *SIAM J. Appl. Math.*, vol. 43, no. 3, pp. 546–552, 1983.

[3] M. Defrise, R. Clack, and D.W. Townsend, "Image reconstruction from truncated, two-dimensional, parallel projections," *Inv. Prob.*, vol. 11, no. 2, pp. 287–313, 1995.

[4] A.A. Kirillov, "On a problem of I.M. Gel'fand," *Sov. Math. Dokl.*, vol. 2, pp. 268-269, 1961.

[5] B.D. Smith, "Image Reconstruction from Cone-Beam Projections: Necessary and Suf cient Conditions and Reconstruction Methods," *IEEE Trans. Med. Imag.*, vol. MI-4, no. 1, 1985.

[6] R.C. Martin, "Designing Object-Oriented C++ Applications Using the Booch Method," Pentice Hall, Englewood Cliffs, 1995.

[7] W.J.T. Spyra, A. Faridani, K.T. Smith, and E.L. Ritman, "Computed Tomographic Imaging of the Coronary Arterial Tree - Use of Local Tomography," *IEEE Trans. Med. Imag.*, vol. 9, no. 1, pp. 1–4, 1990.

[8] F. Natterer, *The Mathematics of Computerized Tomography*, New York: Wiley, 1986.

[9] P. Grangeat,"Mathematical Framework of Cone Beam 3D Reconstruction via the First Derivative of the Radon Transform," in *Mathematical Methods in Tomography (Lecture Notes in Mathematics 1497)*, G. Herman, A.K. Louis, and F. Natterer, Eds. Berlin: Springer, 1991, pp. 66-97.


0-7803-7636-6/03/$17.00 ©2003 IEEE.